Supporting Information for

A comprehensive dataset of luminescence chronologies and environmental proxy indices of loess-paleosol deposits across Asia

Guoqiang Li[1*], Zhongfeng Yan[1], Yougui Song[2*], Kathryn E. Fitzsimmons[3*], Shuangwen Yi[4*], Shugang Kang[2*], Chongyi E[5*], Thomas Stevens[6, 7*], Zhongping Lai[8*], Aditi K. Dave[3, 9*], Chunzhu Chen[10]*, Yanqing Deng[1*], He Yang[11*], Leibin Wang[12] Xiaojian Zhang[4], Caixin Qin[1], Qiuyue Zhao[13], Jan-Pieter Buylaert[14], Tao Lu[15], Yixuan Wang[15], Xiangjun Liu[16], Zhiyong Ling[15], Qiufang Chang[17], Haitao Wei[1], Xiaoyan Wang[1], Fahu Chen[18*]

[1]*Key Laboratory of Western China's Environmental Systems (Ministry of Education), College of Earth and Environmental Sciences, Lanzhou University, Lanzhou 730000, China*

[2]*State Key Laboratory of Loess and Quaternary Geology, Institute of Earth Environment, Chinese Academy of Sciences, Xi'an, China*

[3]*Department of Geosciences, University of Tübingen, Schnarrenbergstrasse 94-96, 72076, Tübingen, Germany*

[4]*School of Geography and Ocean Science, Nanjing University, Nanjing, 210023, China*

[5]*Qinghai Provincial Key Laboratory of Physical Geography and Environmental Processes, School of Geographical Science, Qinghai Normal University, Xining 810008, China*

[6]*Department of Earth Sciences, Uppsala University, Villavagen 16, Uppsala 75236, Sweden*

[7]*Department of Geosciences and Geography, University of Helsinki, P.O. Box 64, 00014, Helsinki, Finland*

[8]*Institute of Marine Sciences, Guangdong Provincial Key Laboratory of Marine Disaster Prediction and Protection, Shantou University, Shantou, Guangdong, 515063, China*

[9]*Interdisciplinary Research Institute on Bionanosciences, Babes Bolyai University, Cluj-Napoca, Romania*

[10]*School of Geographic Science, Nantong University, Nantong 226007, China*

[11]*School of Atmospheric Sciences, Chengdu University of Information Technology, Chengdu 610000, China*

[12]*Centre for Climate and Environmental Changes, School of Geographical Sciences, Guangzhou University, Guangzhou, Guangdong, 510006, China*

[13]*Key Laboratory of Tourism and Resources Environment in Universities of Shandong, Taishan University, 271000, Taian, China*

[14]*Department of Physics, Technical University of Denmark, DTU Risø Campus, Roskilde, Denmark*

[15]*Key Laboratory of Salt Lake Geology and Environment of Qinghai Province, Qinghai Institute of Salt Lakes, Chinese Academy of Sciences, Xining, 810008, China*

[16]*School of Geography and Tourism, Jiaying University, Meizhou, China*

[17]*School of Geography and Tourism, Zhengzhou Normal University, Zhengzhou, China*

[18]*Key Laboratory of Alpine Ecology (LAE), CAS Center for Excellence in Tibetan Plateau Earth Sciences, Institute of Tibetan Plateau Research, Chinese Academy of Sciences (CAS), Beijing 100101, China.*

*Corresponding authors. Guoqiang Li (gqli@lzu.edu.cn), Yougui Song (ygsong@loess.llqg.ac.cn), Kathryn E. Fitzsimmons (kathryn.fitzsimmons@uni-tuebingen.de), Shuangwen Yi (ysw7563@nju.edu.cn), Shugang Kang (kshg@ieecas.cn), Chongyi E (echongyi@163.com), Thomas Stevens (thomas.stevens@geo.uu.se), Zhongping Lai (zhongping_lai@stu.edu.cn), Aditi K. Dave (aditikrishna.dave@gmail.com), Chunzhu Chen (pollenchencz@gmail.com), Yanqing Deng (dengyq19@lzu.edu.cn), He Yang (yanghe@cuit.edu.cn), Fahu Chen (fhchen@itpcas.ac.cn)

This file includes:

Supplementary Figures 1 to 2

Supplementary Table 1

Supplementary Figures

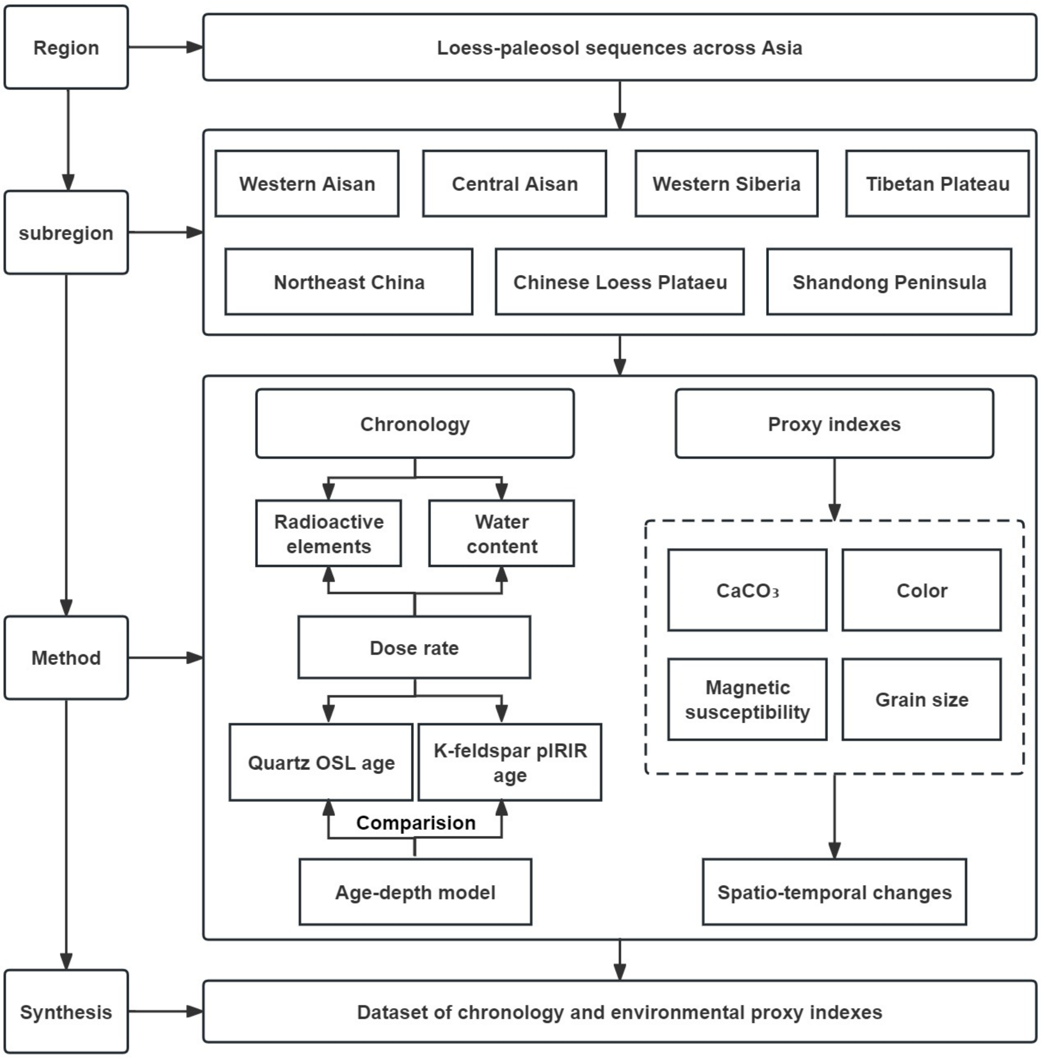

Supplementary Figure 1. Process of constructing the Asian loess dataset, which includes establishing chronology and conducting environmental proxy analysis.

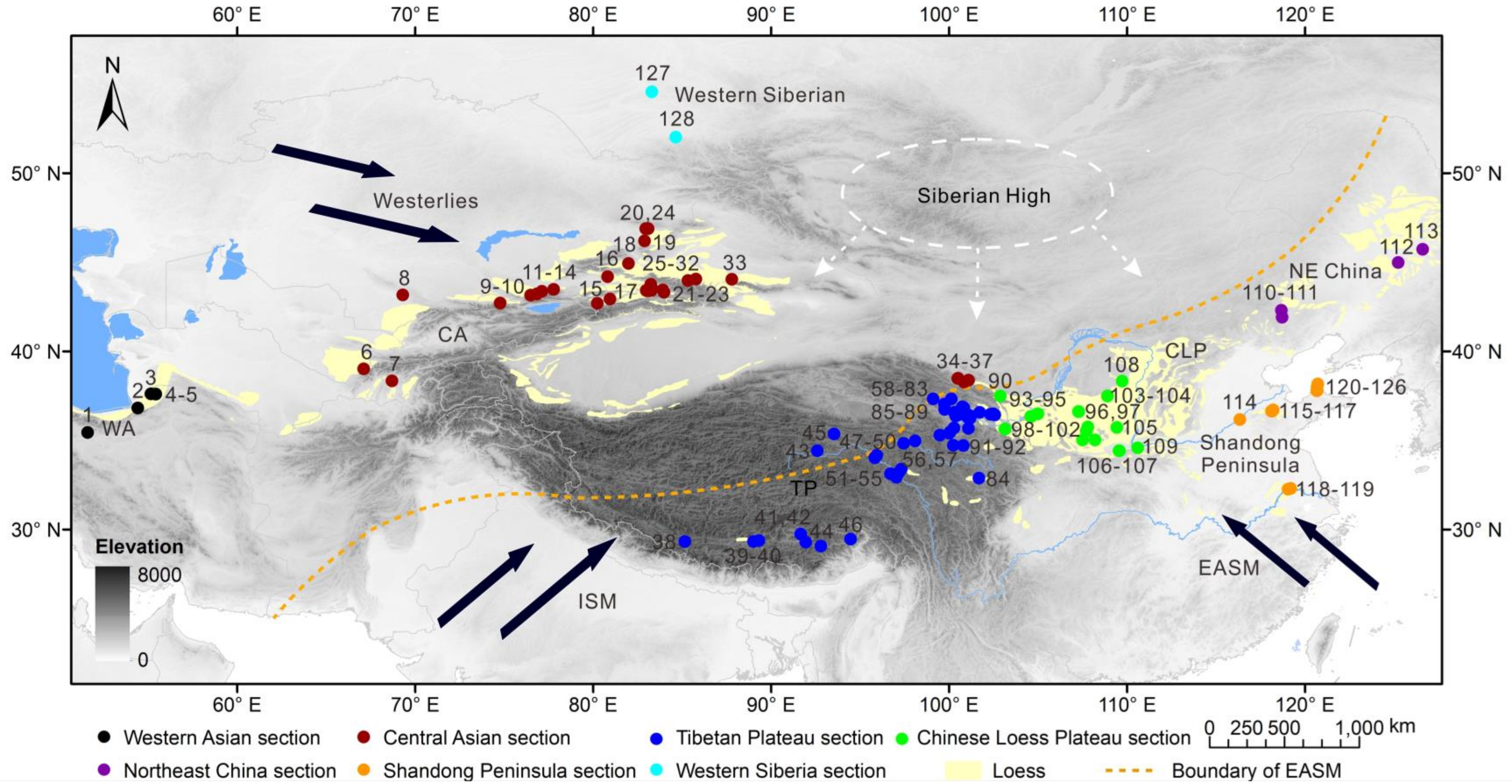

Supplementary Figure 2. The distribution of loess-paleosol sections from Western Asia, Central Asia, Tibetan Plateau, Chinese Loess Plateau, Northeast China, Shandong Peninsula and Western Siberia. The software 91 satellite map (https://www.91weitu.com/) was used to download the DEM data from Google Earth. The map generation were performed in software ArcGIS 10.7.

Supplementary Table 1. The summary of location information and related references for loess-paleosol sections in the dataset.

Number	Section name	Longitude (°E)	Latitude (°N)	Elevation (m)	Depth (m)	Region	Reference
1	Tepe Pardis	51.6	35.45	990	10.5	Western Asia	Gillmore et al., 2011[1]
2	Toshan	54.42	36.82	145	25.7	Western Asia	Lauer et al., 2017a[2]
3	Agh Band	55.16	37.62	183	54	Western Asia	Lauer et al., 2017b[3]
4	YBD	55.43	37.60	383	1.82	Western Asia	Wei et al., 2021[4]
5	YE	55.43	37.60	383	1.24	Western Asia	Wang et al., 2020[5]
6	Rudak	67.12	39.01	1302	6	Central Asia	Zhang et al., 2020b[6]
7	TJK	68.71	38.34	1202	18.2	Central Asia	Tian et al., 2021[7]
8	VAL	69.31	43.17	515	7.5	Central Asia	Fitzsimmons et al., 2017[8]
9	NRO 22	74.78	42.70	1417	10	Central Asia	Youn et al., 2014[9]
10	NRO 1-20	74.78	42.70	1432	20	Central Asia	Youn et al., 2014[9]
11	MBK	76.5	43.15	1040	6	Central Asia	Fitzsimmons et al., 2017[8]
12	REM	76.85	43.22	1070	8	Central Asia	Fitzsimmons et al., 2018[10]; Dave et al., 2023[11]; Schulte et al., 2018[12]
13	PAN	77.13	43.37	710	5	Central Asia	Dave et al., 2023[11];

							Fitzsimmons et al., 2020[13]
14	ASH	77.79	43.48	760	5.1	Central Asia	Dave et al., 2023[11]
15	ZSP	80.25	42.69	1875	6.9	Central Asia	Song et al., 2018a[14]; Song et al., 2018b[15]; Li et al., 2022[16]; Li et al., 2014[17]
16	SGX	80.82	44.19	936	6	Central Asia	Sun et al., 2020[18]
17	ZS	80.96	42.93	1650	3.5	Central Asia	Kang et al., 2020b[19]; 2022b[20]
18	SG18	81.99	44.93	526	23.8	Central Asia	Yang et al., 2021[21]
19	YM	82.9	46.2	/	8.5	Central Asia	Li et al., 2019a[22]
20	TC	82.97	46.88	/	13.4	Central Asia	Li et al., 2019a[22]
21	XEB	82.99	43.42	888	1.4	Central Asia	Kang et al., 2020b[19]; 2022b[20]
22	TLD	83.04	43.40	1020	5.1	Central Asia	Kang et al., 2015[23]; Kang et al., 2020a[24]; Kang et al., 2022a[25]
23	XEBLK	83.07	43.42	1050	30.7	Central Asia	Li et al., 2016[26]
24	KETB	83.11	46.87	850	14	Central Asia	Cheng et al., 2022[27]
25	XY17	83.18	43.40	959	29	Central Asia	Li et al., 2020a[28]
26	NLK	83.25	43.76	1253	20.5	Central Asia	Song et al., 2015[29]; Li et al., 2019b[31]; Li et al.,

							2018[30]
27	ZD17	83.28	43.43	1000	28.5	Central Asia	Yang et al., 2020[32]
28	ZKT	83.31	43.54	900	23	Central Asia	E et al., 2012[33]
29	KS15	83.92	43.46	1370	13	Central Asia	Li et al., 2018[34]
30	NLT17	83.99	43.31	1396	4	Central Asia	Li et al., 2020a[28]
31	LJW10	85.34	43.97	1462	2.8	Central Asia	Li et al., 2015[35]
32	QS16	85.79	44.06	909	44	Central Asia	Li et al., 2020a[28]
33	BYH10	87.80	44.04	622	30	Central Asia	Li et al., 2016[36]
34	CJB21-1	100.51	38.48	2424	11.2	Central Asia	Li et al., 2023[37]
35	CJB21-2	100.51	38.47	2398	3.2	Central Asia	Li et al., 2023[37]
36	BG21-1	100.85	38.28	2743	3.4	Central Asia	Li et al., 2023[37]
37	XG21-1	101.10	38.39	2447	3	Central Asia	Li et al., 2023[37]
38	Sagaxi(SGX)	85.17	29.32	4452	3.6	Tibetan Plateau	Yang et al., 2021[38]
39	YJ1&2	89.02	29.32	3896	10.2	Tibetan Plateau	Chang et al., 2017[39]
40	LCP	89.33	29.39	3815	6.5	Tibetan Plateau	Ling et al., 2020[40]
41	GYA3	91.67	29.75	3840	4	Tibetan Plateau	Lai et al., 2009[41]
42	SNP	91.95	29.28	3598	4.5	Tibetan Plateau	Ling et al., 2020[40]
43	TGL1&2	92.61	34.43	4604	1.6	Tibetan Plateau	Chang et al., 2017[39]
44	LXP	92.80	29.07	3172	2.2	Tibetan Plateau	Ling et al., 2020[40]
45	KKXL1	93.55	35.36	4636	0.48	Tibetan Plateau	Chang et al., 2017[39]
46	YJP1	94.47	29.46	2943	3.6	Tibetan Plateau	Ling et al., 2020[40]
47	QML1	95.83	34.04	4121	2.4	Tibetan Plateau	Huang et al., 2022[42]
48	QML3	95.83	34.04	4133	2	Tibetan Plateau	Huang et al., 2022[42]

49	QML2	95.83	34.04	4175	5	Tibetan Plateau	Huang et al., 2022[42]
50	QML5	95.94	34.16	4605	1.7	Tibetan Plateau	Huang et al., 2022[42]
51	HTS	96.71	33.12	4630	1	Tibetan Plateau	Huang et al., 2022[42]
52	CGS2	97.05	32.94	4087	2.1	Tibetan Plateau	Chang et al., 2017[39]
53	CGS1&3	97.05	32.94	4087	2.6	Tibetan Plateau	Huang et al., 2022[42]
54	HTS2	97.19	33.21	4480	0.85	Tibetan Plateau	Chang et al., 2017[39]
55	ZQX	97.32	33.38	4559	0.9	Tibetan Plateau	Liu et al., 2023[43]
56	ELH1	97.46	34.84	4346	1	Tibetan Plateau	Liu et al., 2023[43]
57	MD3	98.10	34.97	4352	1	Tibetan Plateau	Liu et al., 2023[43]
58	XY18	99.11	37.34	3364	2.8	Tibetan Plateau	Li et al., 2020b[44]
59	XH	99.49	35.30	3542	2.4	Tibetan Plateau	Huang et al., 2022[42]
60	Niaodao	99.74	37.04	3215	6	Tibetan Plateau	E et al., 2019[45]
61	Heimahe	99.76	36.74	3223	2.5	Tibetan Plateau	Zhang et al., 2019[46]
62	NRG	100.01	35.41	/	3.1	Tibetan Plateau	Liu et al., 2017[47]
63	TD	100.07	35.47	3206	3.7	Tibetan Plateau	Huang et al., 2022[42]
64	Gangcha (GC)	100.13	37.33	3305	1.4	Tibetan Plateau	Xue et al., 2021[48]
65	MQ1&2	100.24	34.73	3519	4.05	Tibetan Plateau	Chang et al., 2017[39]
66	Yangqu	100.28	35.70	3000	2	Tibetan Plateau	Yan et al., 2019[49]
67	JXG	100.30	36.58	3291	1.8	Tibetan Plateau	Liu et al., 2012[50]
68	GB065	100.37	36.38	3164	1.3	Tibetan Plateau	Liu et al., 2012[50]
69	QH-18	100.53	36.57	3202	3.6	Tibetan Plateau	Liu et al., 2012[50]
70	XL	100.55	36.45	3518	1.6	Tibetan Plateau	Huang et al., 2022[42]
71	XPS	100.70	36.78	3361	1.68	Tibetan Plateau	Huang et al., 2022[42]

72	Yandongtai	100.76	36.88	3352	/	Tibetan Plateau	Huang et al., 2022[42]
73	Bronze Wire site	100.76	36.88	3344	/	Tibetan Plateau	Huang et al., 2022[42]
74	KTE	100.80	36.75	3340	1.15	Tibetan Plateau	Lu et al., 2015[51]
75	Hebei	100.81	34.72	3669	8	Tibetan Plateau	E et al., 2018[52]
76	KTN	100.83	36.83	3300	3.3	Tibetan Plateau	Lu et al., 2015[51]
77	HK2	100.83	36.48	3250	1.1	Tibetan Plateau	Liu et al., 2012[50]
78	Dongwei	101.04	36.30	3316	3	Tibetan Plateau	E et al., 2019[45]
79	Najiao	101.10	35.67	3629	4	Tibetan Plateau	Xu et al., 2022[53]
80	RYS1	101.11	36.43	3455	2.6	Tibetan Plateau	Zhang et al., 2020a[54]
81	RYS2	101.11	36.43	3429	0.8	Tibetan Plateau	Zhang et al., 2020a[54]
82	RYS17	101.11	36.43	3463	2.2	Tibetan Plateau	Li et al., 2020b[44]
83	Langgeri	101.20	36.25	3565	2.8	Tibetan Plateau	Wei et al., 2020[55]
84	ABa	101.68	32.89	3320	5	Tibetan Plateau	Liu et al., 2023[43]
85	TXD	101.73	36.58	2600	25	Tibetan Plateau	Buylaert et al., 2008[56]
86	LD-1	102.33	36.47	2417	30	Tibetan Plateau	Wang et al., 2018[57]
87	LD-2	102.5	36.5	2300	25	Tibetan Plateau	Buylaert et al., 2008[56]
88	HS	102.58	36.44	1962	12.4	Tibetan Plateau	Wang et al., 2015[58]
89	HS18	102.58	36.43	1970	36.2	Tibetan Plateau	Li et al., 2020b[44]
90	GL	102.88	37.49	2400	20	Chinese Central Loess Plateau	Sun et al., 2012[59]
91	YB02	103.15	35.64	2177	4.5	Chinese Central Loess Plateau	Lai et al., 2006[60]
92	YB03	103.15	35.64	/	18	Chinese Central Loess Plateau	Lai et al., 2007[61]
93	JY12	104.6	36.35	2210	20	Chinese Central Loess Plateau	Sun et al., 2012[59]
94	JY10	104.62	36.35	/	45	Chinese Central Loess Plateau	Sun et al., 2010[62]

95	ZJC	105	36.5	2100	25	Chinese Central Loess Plateau	Buylaert et al., 2008[56]
96	BGY-M	107.28	36.62	1545	12.6	Chinese Central Loess Plateau	Stevens et al., 2006[63]; Stevens et al., 2008[64]
97	BGY-H	107.29	36.62	1523	2.85	Chinese Central Loess Plateau	Stevens et al., 2006[63]
98	Lingtai	107.51	35.02	1340	5.6	Chinese Central Loess Plateau	Perić et al., 2019[65]
99	Xifeng(ZJC)	107.72	35.54	/	5.4	Chinese Central Loess Plateau	Stevens et al., 2016[66]
100	XF06	107.72	35.54	1281	4.3	Chinese Central Loess Plateau	Stevens et al., 2006[63]
101	LGG	107.80	35.76	1070	4.7	Chinese Central Loess Plateau	Kang et al., 2020a[24]
102	Xunyi	108.21	35.02	1151	6.8	Chinese Central Loess Plateau	Stevens et al., 2008[64]
103	Jingbian,A-E	108.90	37.50	/	/	Chinese Central Loess Plateau	Stevens et al., 2018[67]
104	Jingbian	108.91	37.50	1720	6	Chinese Central Loess Plateau	Buylaert et al., 2015[68]
105	LC	109.43	35.73	1108	12.5	Chinese Central Loess Plateau	Lai., 2010[69]
106	WN2	109.56	34.42	646	3.2	Chinese Central Loess Plateau	Kang et al., 2018[70]; 2020a[24]; 2022a[25]
107	WN	109.58	34.43	660	14.28	Chinese Central Loess Plateau	Kang et al., 2011[71]; 2013[72]
108	ZBT	109.73	38.33	1187	16.8	Chinese Central Loess Plateau	Wu et al., 2019[73]
109	GB	110.61	34.58	470	19	Chinese Central Loess Plateau	Kang et al., 2020a[24]; 2022a[25]
110	SBH	118.69	42.30	677	9.7	Northeastern China	Yi et al., 2015[74]
111	NYZG	118.72	41.92	774	3.2	Northeastern China	Yi et al., 2016[75]
112	SY	125.24	44.99	174	5.5	Northeastern China	Wang et al., 2017[76]
113	Huangshan	126.61	45.73	198	30.4	Northeastern China	Wu et al., 2021[77]

114	HeiShan	116.34	36.17	116	7.5	Shandong Peninsula	Zhao et al., 2021[78]
115	Focun-1	118.12	36.64	255	7	Shandong Peninsula	Kong et al., 2021[79]
116	FoCun-2	118.15	36.64	267	6.5	Shandong Peninsula	Zhao et al., 2022[80]
117	ShaoZhuang	118.23	36.72	171	4.5	Shandong Peninsula	Zhao et al., 2022[80]
118	YZ	119.06	32.26	40	18	Shandong Peninsula	Yi et al., 2018[81]
119	MB	119.21	32.31	29	23	Shandong Peninsula	Yi et al., 2018[81]
120	Xiazhupan	120.67	37.79	/	12	Shandong Peninsula	Tian et al., 2019[82]
121	XZP	120.67	37.79	15	7.6	Shandong Peninsula	Miao et al., 2022[83]
122	LGZ	120.69	37.80	5.7	14.5	Shandong Peninsula	Yi et al., 2022[84]
123	Lingezhuang	120.69	37.80	/	15	Shandong Peninsula	Tian et al., 2019[82]
124	Dianzi	120.69	37.99	/	4	Shandong Peninsula	Tian et al., 2019[82]
125	Zouyu	120.71	37.81	/	7.2	Shandong Peninsula	Tian et al., 2019[82]
126	TJD	120.73	38.17	15.3	5.4	Shandong Peninsula	Yi et al., 2022[84]
127	Lozhok	83.31	54.57	165	8.3	Western Siberia	Volvakh et al., 2022[85]
128	Solonovka	84.66	52.02	235	10	Western Siberia	Meshcheryakova et al., 2022[86]

Reference

1. Gillmore, G.K. et al. Geoarchaeology and the value of multidisciplinary palaeoenvironmental approaches: a case study from the Tehran Plain, Iran, Geological society, london, special Publications. 352, 49-67 (2011).
2. Lauer, T. et al. Luminescence-chronology of the loess palaeosol sequence Toshan, Northern Iran – A highly resolved climate archive for the last glacial–interglacial cycle. Quaternary International. 429, 3-12 (2017a).
3. Lauer, T. et al. The Agh Band loess-palaeosol sequence–A terrestrial archive for climatic shifts during the last and penultimate glacial–interglacial cycles in a semiarid region in northern Iran. Quaternary International. 429, 13-30 (2017b).
4. Wei, H.T. et al. Quartz OSL dating of loess deposits since the late glacial in the Southeast of Caspian Sea. Quaternary International. 583, 39-47 (2021).
5. Wang, Q. et al. Holocene moisture variations in western arid central Asia inferred from loess records from NE Iran. Geochemistry, Geophysics, Geosystems. 21, e2019GC008616 (2020).
6. Zhang, J.R., Zhou, X.Y., Long, H. Late Quaternary loess accumulation at the Rudak section in Uzbekistan, central Asia: Chronology and palaeoclimate implications. Palaeogeography, Palaeoclimatology, Palaeoecology. 547, 109695 (2020b).
7. Tian, S.C. et al. Loess deposits in the Tajik Basin, Central Asia: chronology, provenance and palaeoclimatic implications since the Last Glacial. Boreas. 50, 147-166 (2021).

8. Fitzsimmons, K.E. et al. A chronological framework connecting the early Upper Palaeolithic across the Central Asian piedmont. Journal of Human evolution. 113, 107-126 (2017).

9. Youn, J. H., Seong, Y. B., Choi, J. H., Abdrakhmatov, K., Ormukov, C. Loess deposits in the northern Kyrgyz Tien Shan: Implications for the paleoclimate reconstruction during the Late Quaternary. Catena. 117, 81-93 (2014).

10. Fitzsimmons, K.E. et al. Loess accumulation in the Tian Shan piedmont: Implications for palaeoenvironmental change in arid Central Asia. Quaternary international. 469, 30-43 (2018).

11. Dave, A.K., Lisa, L., Scardia, G., Nigmatova, S., and Fitzsimmons, K.E. The patchwork loess of Central Asia: Implications for interpreting aeolian dynamics and past climate circulation in piedmont regions. Journal of Quaternary Science. 38(4), 526-543 (2023).

12. Schulte, P., Sprafke, T., Rodrigues, L., Fitzsimmons, K.E. Are fixed grain size ratios useful proxies for loess sedimentation dynamics? Experiences from Remizovka, Kazakhstan. Aeolian research. 31, 131-140 (2018).

13. Fitzsimmons, K.E., Nowatzki, M., Dave, A.K., Harder, H. Intersections between wind regimes, topography and sediment supply: Perspectives from aeolian landforms in Central Asia. Palaeogeography, Palaeoclimatology, Palaeoecology. 540, 109531 (2020).

14. Song, Y.G. et al. Radiometric dating of late Quaternary loess in the northern piedmont of South Tianshan Mountains: Implications for reliable dating.

Geological Journal. 53, 417-426 (2018a).

15. Song, Y.G. et al. Abrupt climatic events recorded by the Ili loess during the last glaciation in Central Asia: Evidence from grain-size and minerals. Journal of Asian Earth Sciences. 155, 58-67 (2018b).
16. Li, Y.D. et al. Effective Moisture Evolution since the Last Glacial Maximum Revealed by a Loess Record from the Westerlies-Dominated Ili Basin, NW China. Atmosphere. 13, 1931 (2022).
17. Li, Y., Song, Y.G., Wang, Q.S. Chroma characteristics in the Zhaosu loess section and its paleoclimatic significance. Journal of Earth Environment. 5, 67-75 (2014).
18. Sun, H.Y., Song, Y.G., Chen, X.L., Cheng, L.Q., Liu, H.F. Holocene dust deposition in the Ili Basin and its implications for climate variations in Westerlies-dominated Central Asia. Palaeogeography, Palaeoclimatology, Palaeoecology. 550, 109731 (2020).
19. Kang, S.G. et al. Increasing effective moisture during the Holocene in the semiarid regions of the Yili Basin, Central Asia: Evidence from loess sections. Quaternary Science Reviews. 246, 106553 (2020b).
20. Kang, S.G. et al. Siberian High Modulated Suborbital-Scale Dust Accumulation Changes Over the Past 30 ka in the Eastern Yili Basin, Central Asia. Paleoceanography and Paleoclimatology. 37, e2021PA004360 (2022b).
21. Yang, H. et al. The close-space luminescence dated loess record from SW Junggar Basin indicates persistent aridity during the last glacial-interglacial cycle in lowlands of Central Asia. Palaeogeography, Palaeoclimatology, Palaeoecology.

584, 110664 (2021).

22. Li, Y., Song, Y.G., Yin, Q.Z., Han, L., Wang, Y.X. Orbital and millennial northern mid-latitude westerlies over the last glacial period. Climate Dynamics. 53, 3315-3324 (2019a).

23. Kang, S.G., Roberts, H.M., Wang, X.L., An, Z.S., Wang, M. Mass accumulation rate changes in Chinese loess during MIS 2, and asynchrony with records from Greenland ice cores and North Pacific Ocean sediments during the Last Glacial Maximum. Aeolian Research. 19, 251-258 (2015).

24. Kang, S.G. et al. Early Holocene weakening and mid-to late Holocene strengthening of the East Asian winter monsoon. Geology. 48, 1043-1047 (2020a).

25. Kang, S.G., Wang, X.L., Du, J.H., Song, Y.G. Paleoclimates inform on a weakening and amplitude-reduced East Asian winter monsoon in the warming future. Geology. 50, 1224-1228 (2022a).

26. Li, G.Q. et al. Paleoenvironmental changes recorded in a luminescence dated loess/paleosol sequence from the Tianshan Mountains, arid central Asia, since the Penultimate Glaciation. Earth and Planetary Science Letters. 448, 1-12 (2016).

27. Cheng, L.G. et al. Variations of the Intensity of the Siberian High During the Last Glacial Revealed by the Sorting Coefficient of Loess-Paleosol Deposits in Eastern Central Asia. Paleoceanography and Paleoclimatology. 37, e2022PA004468 (2022).

28. Li, G.Q. et al. Differential ice volume and orbital modulation of Quaternary moisture patterns between Central and East Asia. Earth and Planetary Science

Letters. 530, 115901 (2020a).

29. Song, Y.G., Lai, Z.P., Li, Y., Chen, T., Wang, Y.X. Comparison between luminescence and radiocarbon dating of late Quaternary loess from the Ili Basin in Central Asia. Quaternary Geochronology. 30, 405-410 (2015).
30. Li, Y. et al. Eolian dust dispersal patterns since the last glacial period in eastern Central Asia: insights from a loess-paleosol sequence in the Ili Basin. Climate of the Past. 14, 271-286 (2018).
31. Li, Y., Song, Y.G., Qiang, M.R., Miao, Y.F., Zeng, M.X. Atmospheric dust variations in the Ili Basin, Northwest China, during the last glacial period as revealed by a high Mountain Loess-paleosol sequence. Journal of Geophysical Research Atmospheres. 124, 8449-8466 (2019b).
32. Yang, H. et al. Loess depositional dynamics and paleoclimatic changes in the Yili Basin, Central Asia, over the past 250 ka. Catena. 195, 104881 (2020).
33. E, C.Y. et al. A luminescence dating study of loess deposits from the Yili River basin in western China. Quaternary Geochronology. 10, 50-55 (2012).
34. Li, G.Q. et al. A Tianshan Mountains loess-paleosol sequence indicates anti-phase climatic variations in arid central Asia and in East Asia. Earth and Planetary Science Letters. 494, 153-163 (2018).
35. Li, G.Q. et al. Quartz OSL and K-feldspar pIRIR dating of a loess/paleosol sequence from arid central Asia, Tianshan Mountains, NW China. Quaternary Geochronology. 28, 40-53 (2015).
36. Li, Y., Song, Y.G., Lai, Z.P., Han, L., An, Z.S. Rapid and cyclic dust accumulation

during MIS 2 in Central Asia inferred from loess OSL dating and grain-size analysis. Scientific Reports. 6, 32365 (2016).

37. Li, G.Q. et al. High-resolution luminescence chronology of loess-paleosols reveals East Asian summer monsoon and winter monsoon variation in Hexi Corridor during the past 25 kyr. Palaeogeography, Palaeoclimatology, Palaeoecology. 627, 111743 (2023).
38. Yang, J.H. et al. Holocene moisture evolution and its response to atmospheric circulation recorded by aeolian deposits in the southern Tibetan Plateau. Quaternary Science Reviews. 270, 107169 (2021).
39. Chang Q.F. Photochronology and Environmental Significance of Aeolian Deposits on the Qinghai-Tibet Plateau and the Nalingele River Terrace, University of Chinese Academy of Sciences. Qinghai Salt Lake Research Institute of Chinese Science (2017).
40. Ling, Z.Y. et al. Spatial-temporal differentiation of eolian sediments in the Yarlung Tsangpo catchment, Tibetan Plateau, and response to global climate change since the Last Glaciation. Geomorphology. 357, 107104 (2020).
41. Lai, Z.P., Kaiser, K., Brückner, H. Luminescence-dated aeolian deposits of late Quaternary age in the southern Tibetan Plateau and their implications for landscape history. Quaternary Research. 72, 421-430 (2009).
42. Huang, X.M. et al. Tibetan dust accumulation linked to ecological and landscape response to global climate change. Geophysical Research Letters. 49, e2021GL096615 (2022).

43. Liu, X.J. et al. Distribution and fate of Tibetan Plateau loess. Catena. 225, 107022 (2023).

44. Li, G.Q. et al. Paleoclimatic changes and modulation of East Asian summer monsoon by high-latitude forcing over the last 130,000 years as revealed by independently dated loess-paleosol sequences on the NE Tibetan Plateau. Quaternary Science Reviews. 237, 106283 (2020b).

45. E, C.Y. et al. High resolution OSL dating of aeolian activity at Qinghai Lake, Northeast Tibetan Plateau. Catena. 183, 104180 (2019).

46. Zhang, J., E, C.Y., Zhao, Y.J. High density photoluminescence dating of the Heimahe loess in Qinghai Lake. Journal of the Earth Environment. 9, 557-568 (2019).

47. Liu, X.J. et al. Accumulation and erosion of aeolian sediments in the northeastern Qinghai-Tibetan Plateau and implications for provenance to the Chinese Loess Plateau. Journal of Asian Earth Sciences. 135, 166-174 (2017).

48. Xue, H., Zeng, F. Holocene environmental evolution in the Qinghai Lake area recorded by aeolian deposits. Quaternary International. 580, 67-77 (2021).

49. Yan, W.T. et al. Study on the history of wind sand activity in the Gonghe Basin based on photoluminescence dating. Salt Lake Research. 27, 28-38 (2019).

50. Liu, X.J., Lai, Z.P., Yu, L.P., Sun, Y.J., Madsen, D. Luminescence chronology of aeolian deposits from the Qinghai Lake area in the Northeastern Qinghai-Tibetan Plateau and its palaeoenvironmental implications. Quaternary Geochronology. 10, 37-43 (2012).

51. Lu, R.J. et al. Holocene aeolian activity and climatic change in Qinghai Lake basin, northeastern Qinghai–Tibetan Plateau. Palaeogeography, Palaeoclimatology, Palaeoecology. 430, 1-10 (2015).
52. E, C.Y. et al. Hebei loess section in the Anyemaqen Mountains, northeast Tibetan Plateau: a high-resolution luminescence chronology. Boreas. 47, 1170-1183 (2018).
53. Xu, C.X. et al. Holocene Aeolian Activity Recorded by Mountain Paleosols, Gonghe Basin, Northeast Qinghai-Tibet Plateau. Frontiers in Earth Science. 10, 89 (2022).
54. Zhang, J. et al. An alpine meadow soil chronology based on OSL and radiocarbon dating, Qinghai Lake, northeastern Tibetan Plateau. Quaternary International. 562, 35-45 (2020a).
55. Wei, H.C. et al. Climate change and anthropogenic activities in Qinghai Lake basin over the last 8500 years derived from pollen and charcoal records in an aeolian section. Catena. 193, 104616 (2020).
56. Buylaert, J. P. et al. Optical dating of Chinese loess using sand-sized quartz: Establishing a time frame for Late Pleistocene climate changes in the western part of the Chinese Loess Plateau. Quaternary Geochronology. 3, 99-113 (2008).
57. Wang, Y.X. et al. Quartz OSL and K-feldspar post-IR IRSL dating of loess in the Huangshui river valley, northeastern Tibetan plateau. Aeolian Research. 33, 23-32 (2018).
58. Wang, X.Y.et al. Aeolian process and climatic changes in loess records from the

northeastern Tibetan Plateau: Response to global temperature forcing since 30 ka. Paleoceanography. 30, 612-620 (2015).

59. Sun, Y.B. et al. Influence of Atlantic meridional overturning circulation on the East Asian winter monsoon. Nature Geoscience. 5, 46-49 (2012).
60. Lai, Z.P., Wintle, A.G. Locating the boundary between the Pleistocene and the Holocene in Chinese loess using luminescence. The Holocene. 16, 893-899 (2006).
61. Lai, Z.P., Wintle, A.G., Thomas, D.S.G. Rates of dust deposition between 50 ka and 20 ka revealed by OSL dating at Yuanbao on the Chinese Loess Plateau. Palaeogeography, Palaeoclimatology, Palaeoecology. 248, 431-439 (2007).
62. Sun, Y.B., Wang, X.L., Liu, Q.S., Clemens, S. C. Impacts of post-depositional processes on rapid monsoon signals recorded by the last glacial loess deposits of northern China. Earth and Planetary Science Letters. 289, 171-179 (2010).
63. Stevens, T., Armitage, S.J., Lu, H.Y., Thomas, D.S.G. Sedimentation and diagenesis of Chinese loess: implications for the preservation of continuous high-resolution climate records. Geology. 34, 849-852 (2006).
64. Stevens, T., Lu, H.Y., Thomas, D. S., Armitage, S. J. Optical dating of abrupt shifts in the late Pleistocene East Asian monsoon. Geology. 36, 415-418 (2008).
65. Perić, Z. et al. Quartz OSL dating of late quaternary Chinese and Serbian loess: a cross Eurasian comparison of dust mass accumulation rates. Quaternary International. 502, 30-44 (2019).
66. Stevens, T. et al. Mass accumulation rate and monsoon records from Xifeng, Chinese Loess Plateau, based on a luminescence age model. Journal of Quaternary

Science. 31, 391-405 (2016).

67. Stevens, T. et al. Ice-volume-forced erosion of the Chinese Loess Plateau global Quaternary stratotype site. Nature Communications. 9, 983 (2018).

68. Buylaert, J.P. et al. A detailed post-IR IRSL chronology for the last interglacial soil at the Jingbian loess site (northern China). Quaternary Geochronology. 30, 194-199 (2015).

69. Lai, Z.P. Chronology and the upper dating limit for loess samples from Luochuan section in the Chinese Loess Plateau using quartz OSL SAR protocol. Journal of Asian Earth Sciences. 37, 176-185 (2010).

70. Kang, S.G. et al. Late Holocene anti-phase change in the East Asian summer and winter monsoons. Quaternary Science Reviews. 188, 28-36 (2018).

71. Kang, S.G., Lu, Y.C., Wang, X.L. Closely-spaced recuperated OSL dating of the last interglacial palaeosol in the southeastern margin of Chinese Loess Plateau. Quaternary Geochronology. 6, 480-490 (2011).

72. Kang, S.G., Wang, X.L., Lu, Y.C. Quartz OSL chronology and dust accumulation rate changes since the Last Glacial at Weinan on the southeastern Chinese Loess Plateau. Boreas. 42, 815-829 (2013).

73. Wu, J. et al. Establishing a high-resolution luminescence chronology for the Zhenbeitai sand-loess section at Yulin, North-Central China. Quaternary Geochronology. 49, 78-84 (2019).

74. Yi, S.W. et al. High resolution OSL and post-IR IRSL dating of the last interglacial-glacial cycle at the Sanbahuo loess site (northeastern China). Quaternary

Geochronology. 30, 200-206 (2015).

75. Yi, S.W. et al. A detailed post-IR IRSL dating study of the Niuyangzigou loess site in northeastern China. Boreas. 45, 644-657 (2016).

76. Wang, S.N., Wang, X.L., Kang, S.G. A preliminary study on the luminescence dating of the Songyuan loess during the last glacial period in Northeast China and its paleoclimatic significance. Journal of the Earth Environment. 8, 397-406 (2017).

77. Wu, P. et al. Loess accumulation in Harbin with implications for Late Quaternary aridification in the Songnen Plain, Northeast China. Palaeogeography, Palaeoclimatology, Palaeoecology. 570, 110365 (2021).

78. Zhao, Q.Y. et al. High resolution quartz OSL and K-feldspar post-IR IRSL dating of loess in the central Shandong Mountains (Eastern China). Geochronometria. 48, 232-241 (2021).

79. Kong, F.B. et al. Application of grain size endmember analysis in the study of dust accumulation processes: A case study of loess in Shandong Province, East China. Sedimentary Geology. 416 (2021).

80. Zhao, Q.Y. et al. Luminescence chronology of loess-palaeosol deposits in the Central Shandong Mountains region: Provenances and paleoclimate implications. Quaternary Geochronology. 70, 101296 (2022).

81. Yi, S.W. et al. High resolution luminescence chronology for Xiashu Loess deposits of Southeastern China. Journal of Asian Earth Sciences. 155, 188-197 (2018).

82. Tian, S.C. et al. Optically stimulated luminescence dating of late Quaternary loess

deposits in the coastal region of North China: Provenance and paleoclimatic implications. Quaternary Science Reviews. 218, 160-177 (2019).

83. Miao, X.D. et al. Age and source of coastal loess in Shandong Peninsula, Bohai Sea, China: Implications for dust aggradation in respond to sea-level change. Aeolian Research. 54, 100767 (2022).

84. Yi, S.W. et al. Sea-level changes in the Bohai Sea, northern China, constrained by coastal loess accumulation over the past 200 ka. Quaternary Science Reviews. 277, 107368 (2022).

85. Volvakh, N.E. et al. First high-resolution luminescence dating of loess in Western Siberia. Quaternary Geochronology. 73, 101377 (2022).

86. Meshcheryakova, O.A. et al. The upper Pleistocene loess-palaeosol sequence at solonovka on the Cis-Altai plain, west Siberia-First luminescence dating results. Quaternary Geochronology. 73 (2022).